Matrix Isolation and Ab Initio Study of the Noncovalent Complexes between Formamide and Acetylene

Artur Mardyukov, Elsa Sánchez-García, and Wolfram Sander*

Lehrstuhl für Organische Chemie II der Ruhr-Universität Bochum, D-44780 Bochum, Germany

Received: July 28, 2008; Revised Manuscript Received: October 18, 2008

Matrix isolation spectroscopy in combination with ab initio calculations is a powerful technique for the identification of weakly bound intermolecular complexes. Here, weak complexes between formamide and acetylene are studied, and three 1:1 complexes with binding energies of −2.96, −2.46, and −1.79 kcal/mol have been found at the MP2 level of theory (MP2/cc-pVTZ + ZPE + BSSE). The two most stable dimers **A** and **B** are identified in argon and nitrogen matrices by comparison between the experimental and calculated infrared frequencies. Both complexes are stabilized by the formamide C═O···HC acetylene and H···π interactions. Large shifts have been observed experimentally for the C−H stretching vibrations of the acetylene molecule, in very good agreement with the calculated values. Eight 1:2 FMA−acetylene trimers (T-**A** to T-**H**) with binding energies between −5.44 and −2.62 kcal/mol (MP2/aug-cc-pVDZ + ZPE + BSSE) were calculated. The two most stable trimers T-**A** and T-**B** are very close in energy and have similar infrared spectra. Several weak bands that are in agreement with the calculated frequencies of the trimers T-**A** and T-**B** are observed under matrix isolation conditions. However, the differences are too small for a definitive assignment.

Introduction

Amides play an essential role in biochemistry and organic chemistry. Formamide (FMA) is the simplest molecule containing the amide bond, which is the basis of peptide chemistry.[1,2] The structure and spectroscopic properties of FMA have been studied in detail. The monomer and dimers of FMA in inert gas matrices were studied by Räsänen.[3,4] The interactions of FMA with water,[5] hydrogen fluoride,[6] and the isocyanat anion[7] have been studied using matrix isolation spectroscopy and ab initio methods. Selective UV irradiation of the isolated FMA monomer in an argon matrix at 193 nm leads to the formation of the CO···NH_3 and HNCO···H_2 complexes as photoproducts.[8] Alternatively, the UV irradiations at 248 nm in an argon matrix produces formimidic acid (H(OH)C═NH), a tautomer of FMA.[9]

The weak CH···O and CH···π interactions have gained more attention in recent years because of their significant role in determining the shapes and stabilities of proteins and crystal structures. The CH···X complexes, where X can be a proton acceptor such as O, N, halogens, or a π system, have been studied experimentally and theoretically.[10−12] Ault and coworkers[13−15] extensively studied the hydrogen-bonded complexes of alkynes and alkenes with several oxygen and nitrogen atom-containing bases by the matrix isolation technique. Acetylene (Ac) is of special interest to study intermolecular interactions since this hydrocarbon contains relatively acidic hydrogen atoms, which can act as hydrogen bond donors as well as an extended π-system as a hydrogen bond acceptor. It is thus an ideal probe to investigate the capability of polar molecules to form intermolecular bonds. Here, we describe the formation of dimers and trimers between FMA and Ac (FMA−Ac) using infrared matrix isolation spectroscopy and ab initio calculations.

Experimental Details

Matrix Isolation. Matrix isolation experiments were performed by standard techniques using closed-cycle helium refrigerators. The FMA was distilled two times, dried over molecular sieve and degassed several times by the freeze−pump−thaw method before mixing it with argon. FMA−Ac mixtures were prepared by standard manometric techniques. To obtain the necessary vapor pressure of FMA, the gas mixture was kept at 80 °C. About 0.2−0.5 mbar of FMA was mixed with 0.2−1 mbar of Ac and diluted with 600−800 mbar of argon in a 2 L flask. Approximately 30 mbar of the gas mixture was deposited on a CsI substrate at 9 K within 50 min. The matrix was annealed up to 40 K and cooled back to 9 K before recording the spectra. The spectra were recorded on a Fourier transform infrred (FTIR) spectrometer with 0.5 cm^{-1} resolution in the range of 400−4000 cm^{-1}.

Computational Methods. The multiple minima hypersurface (MMH) approach[16−21] was used for searching the minima of the FMA−Ac dimers and the trimers formed by one molecule of FMA and two molecules of Ac. One thousand randomly arranged FMA−Ac dimers and 200 trimers were generated as starting points, and the resulting geometries were optimized and analyzed using the PM3 and AM1[22−25] semiempirical quantum mechanical Hamiltonians.

These semiempirical results provided a preliminary overview of the FMA−Ac interactions, and the relevant configurations were further refined using second-order Møller−Plesset perturbation theory (MP2).[26] Pople's 6-31G(d,p) basis set,[27,28] and augmented and nonaugmented Dunning's correlation consistent double and triple ζ basis sets[29] (aug-cc-pVDZ and cc-pVTZ, the triple-ζ only for dimers) were used for tight geometry optimizations and calculation of the vibrational spectra.

The ab initio computations were performed using the Gaussian 98[30] and Gaussian 03[31] programs. The stabilization energies were calculated by subtracting the energies of the monomers

* To whom correspondence should be addressed.

10.1021/jp806675n CCC: $40.75
Published on Web 01/21/2009

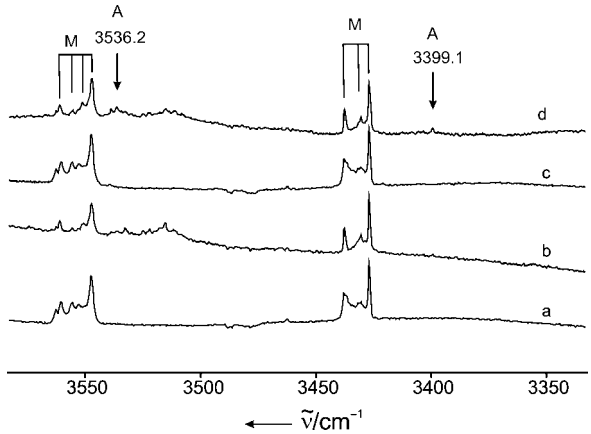

Figure 1. IR spectra in the range 3550−3350 cm^{-1} of FMA/Ac mixtures matrix-isolated in argon: (a) FMA/Ac/Ar ratio 1:1:600, 10 K; (b) FMA/Ac/Ar ratio 1:1:600, after annealing at 30 K; (c) FMA/Ac/Ar ratio 1:3:600, 10 K; (d) FMA/Ac/Ar ratio 1:3:600 after annealing at 30 K.

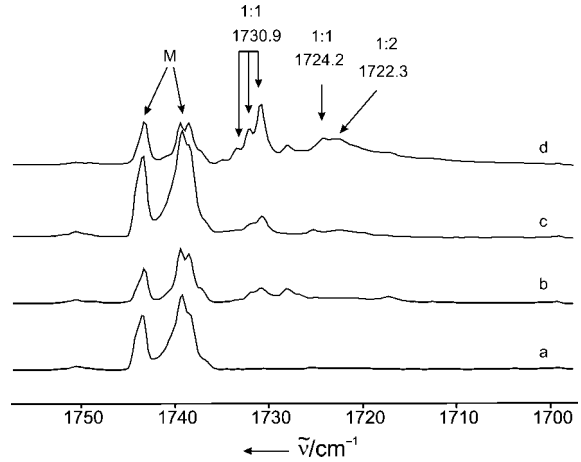

Figure 2. IR spectra in the range 1760−1700 cm^{-1} of FMA/Ac mixtures matrix-isolated in argon: (a) FMA/Ac/Ar ratio 1:1:600, 10 K; (b) FMA/Ac/Ar ratio 1:1:600, after annealing at 30 K; (c) FMA/Ac/Ar ratio 1:3:600, 10 K; (d) FMA/Ac/Ar ratio 1:3:600 after annealing at 30 K.

from those of the complexes and including ZPE corrections. All the energies, including those of the trimers were also corrected for the basis set superposition errors (BSSE) using the counterpoise (CP) scheme of Boys and Bernardi.[32]

Results and Discussion

Experimental Results. The matrix isolation of FMA as well as of Ac has been studied by several groups.[3,4,33−39] Our reference infrared spectra of FMA and Ac in argon and nitrogen matrices are in good agreement with the data reported in literature. Mixed aggregates (mainly dimers) were produced by matrix isolation of mixtures of FMA and Ac in argon or nitrogen at 10 K and subsequent annealing of these matrices at temperatures up to 40 K. Under the conditions of high dilution in either argon or nitrogen and slow deposition of the matrices at 10 K, mainly the monomers of FMA and Ac are isolated. At 10 K these matrices are very rigid, and the diffusion of trapped molecules is efficiently inhibited, whereas, at higher temperatures (approximately 1/3 of the melting point of the matrices), small molecules start to diffuse, and intermolecular reactions become possible. This technique allows us to directly monitor the aggregation via IR spectroscopy.

Argon Matrix. The asymmetric and symmetric N−H stretching modes of FMA are strongly affected by the formation of complexes (Figure 1). In the presence of both FMA and Ac in argon, new bands are observed at 3536.2 and 3399.1 cm^{-1} assigned to FMA−Ac complexes. Compared to the unperturbed N−H stretching vibrations of the FMA monomer at 3547.4 and 3426.6 cm^{-1}, these bands are red-shifted by 11.2 and 27.5 cm^{-1}, respectively. The additional band at 3521.6 cm^{-1} is due to the symmetrical FMA dimer.

The C═O stretching vibration of FMA shows also characteristic shifts induced by the formation of FMA−Ac complexes (Figure 2). The band at 1739.1 cm^{-1} is assigned to the C═O stretching vibration of the FMA monomer.[3] Matrix site effects cause a splitting of this band. After annealing the matrix at 30 K for several minutes, new absorptions appear at 1730.9, 1724.2, and 1722.3 cm^{-1}. These bands are red-shifted by 8.2, 14.9, and 16.8 cm^{-1}, respectively, compared to the C═O stretching vibration of the FMA monomer. Increasing the Ac concentration and annealing the matrix for several minutes to allow diffusion of the trapped species results in an increase of the intensity of these bands. Since the new bands appear only in the presence of both FMA and Ac, they are assigned to FMA−Ac complexes. The peaks at 1730.9 cm^{-1} and 1724.2 cm^{-1} are also observed at low concentrations of either FMA or Ac, and therefore are assigned to dimers of FMA−Ac and not to higher aggregates. The additional band at 1728.0 cm^{-1} belongs to the symmetrical FMA dimer.

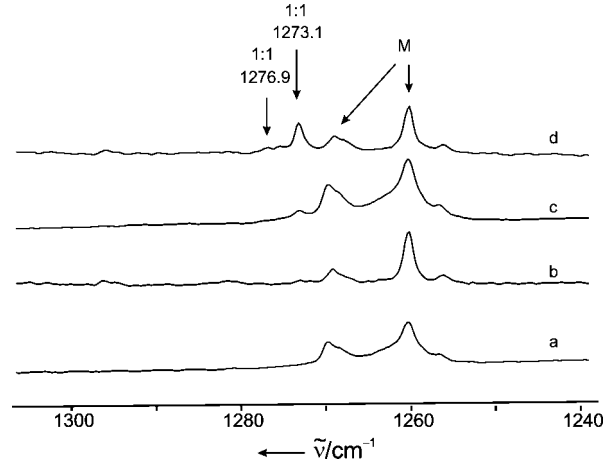

Figure 3. IR spectra in the range 1300−1240 cm^{-1} of FMA/Ac mixtures matrix-isolated in argon: (a) FMA/Ac/Ar ratio 1:1:600, 10 K; (b) FMA/Ac/Ar ratio 1:1:600, after annealing at 30 K; (c) FMA/Ac/Ar ratio 1:3:600, 10 K; (d) FMA/Ac/Ar ratio 1:3:600 after annealing at 30 K.

The doublet peaks at 1269.8 and 1260.4 cm^{-1} (Figure 3) correspond to the C−N stretching vibration of the FMA monomer. A blue shift of the C−N stretching vibration is characteristic of FMA in hydrogen-bonded complexes.[5,6] After annealing the matrix for several minutes at 30 K, a new band at 1273.1 cm^{-1} appears; simultaneously, the monomer bands start to decrease. On codeposition of FMA with Ac and Ar (1:3:600 molar ratios), the peak at 1273.1 cm^{-1} can be observed even without annealing (Figure 3, spectrum c). After annealing the matrix at 30 K, this band gains in intensity, as expected for a FMA−Ac complex. Even at low concentrations of FMA or Ac, the peak at 1273.1 cm^{-1} is found, and is therefore assigned to the C−N stretching mode of a 1:1 FMA−Ac complex. Another weak band is observed at 1276.9 cm^{-1}, blue-shifted by 16.5 cm^{-1} from the unperturbed FMA. The band at 1296.0 is assigned to the FMA dimer.

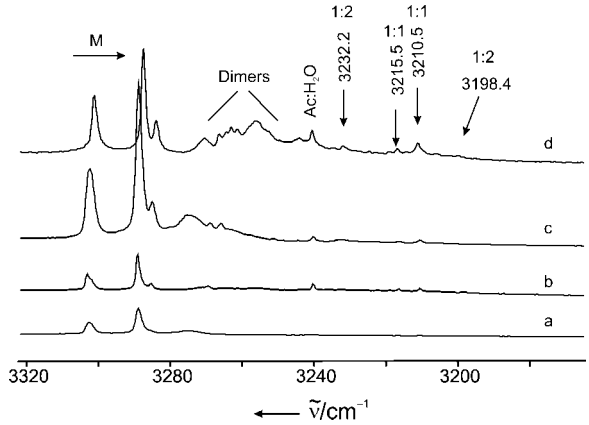

Figure 4. IR spectra in the range 3200−3180 cm^{-1} of FMA/Ac mixtures matrix-isolated in argon: (a) FMA/Ac/Ar ratio 1:1:600, 10 K; (b) FMA/Ac/Ar ratio 1:1:600, after annealing at 30 K; (c) FMA/Ac/Ar ratio 1:3:600, 10 K. (d) FMA/Ac/Ar ratio 1:3:600 after annealing at 30 K.

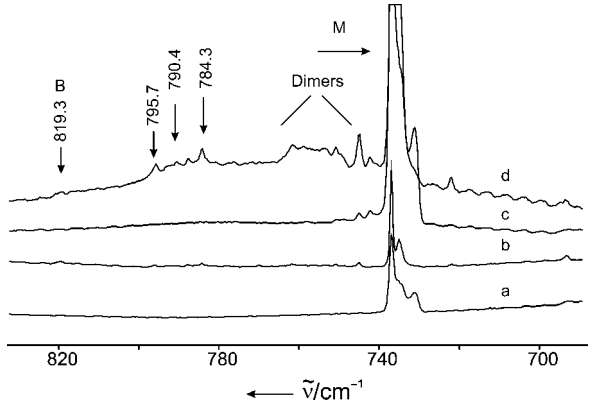

Figure 5. IR spectra in the range 830−700 cm^{-1} of FMA/Ac mixtures matrix-isolated in argon: (a) FMA/Ac/Ar ratio 1:1:600, 10 K; (b) FMA/Ac/Ar ratio 1:1:600, after annealing at 30 K; (c) FMA/Ac/Ar ratio 1:3:600, 10 K. (d) FMA/Ac/Ar ratio 1:3:600 after annealing at 30 K (see Tables 4, 5, and 6).

The vibrational modes of Ac are also perturbed in the presence of FMA. The C−H stretching mode (ν_3) of the Ac monomer is observed at 3288.8 cm^{-1}, and the ($\nu_2 + \nu_4 + \nu_5$) mode is observed at 3302.9 cm^{-1}.[34] Additional weak bands found around 3285, 3269, and 3265 cm^{-1} are assigned to Ac dimers (Figure 4).[34,35,37] The weak band at 3240 cm^{-1} has been assigned to a complex between Ac and water by Engdahl and Nelander.[40] When Ac and FMA are codeposited, new bands are observed at 3205.5, 3210.5, 3215.5, and 3232.2 cm^{-1}. The intensity of these absorptions depends on the FMA concentration, indicating the formation of FMA−Ac complexes. In the CCH bending region of Ac, the doubly degenerated ν_5 mode is observed at 736.8 cm^{-1} with two satellites at 744.7 and 750.8 cm^{-1} (Figure 5).[35,36] After codeposition of FMA with Ac, new bands appear at 784.3, 790.4, 795.7, and 819.3 cm^{-1}. The intensities of these absorptions increase with increasing concentrations of both FMA and Ac, and are thus assigned to 1:1 complexes.

Nitrogen Matrix. To investigate the influence of the matrix host, the FMA/Ac experiments were also performed in nitrogen matrices. In the N−H stretching region, the strong bands at 3553.2 and 3430.5 cm^{-1} are assigned to the asymmetric and symmetric N−H stretching modes of the FMA monomer, in good agreement with the values previously reported by Räsänen.[3] The bands at 3517.6, 3513.9, and 3511.7 cm^{-1} are due to the formation of FMA dimers in the nitrogen matrix (Figure 6).[4]

In the presence of both FMA and Ac, new bands are observed at 3540.7, 3428.4, and 3405.7 cm^{-1}. The intensities of these bands increase with the concentration of both FMA and Ac, indicating the formation of 1:1 complexes.

In the nitrogen matrix, the C═O stretching mode of the FMA monomer appears at 1736.1 cm^{-1} (Figure 7).[3] In the presence of both FMA and Ac, new bands appear at 1729.3, 1726.0, and 1721.9 cm^{-1}, which are assigned to the C═O stretching vibrations of FMA−Ac complexes. The bands at 1729.3 and 1726.0 cm^{-1} can be observed at low concentrations of Ac and FMA and are thus assigned to dimers and not to higher aggregates. In contrast, the band at 1721.9 cm^{-1} appears only at high concentrations of Ac. Therefore, this band can be assigned to a 1:2 FMA−Ac complex.

A few new bands are observed in the region of C−N stretching vibrations of FMA at 1274.9, 1267.5, and 1260.8 cm^{-1}(Figure 8). These bands are blue-shifted from the unperturbed C−N stretching vibration mode at 1246.5 cm^{-1}.

The unperturbed C−H stretching vibration of Ac in solid nitrogen appears at 3283.0 cm^{-1} and 3311.0 cm^{-1}, the latter with very low intensity.[36] Bands at 3218.5 and 3225.7 cm^{-1} are assigned to the Ac−H_2O complex, and bands at 3258.0 and 3279.2 cm^{-1} are assigned to the Ac dimer.[41]

When Ac and FMA are codeposited in nitrogen and the matrix is subsequently annealed, new bands appear at 3226.1, 3221.4, and (barely visible at) 3215.5 cm^{-1}. These bands correspond to the ν_3 stretching vibration of Ac in FMA−Ac complexes (Figure 9).

The CC−H bending mode occurs as a doublet at 747.6 and 742.1 cm^{-1} (Figure 10).[36] After codeposition of FMA with Ac, new bands at 796.4, 791.1, and 787.7 cm^{-1} are observed. From the dependence of the intensities of these absorptions on the concentrations of both monomers, we conclude that 1:1 complexes of FMA and Ac are formed.

TABLE 1: Calculated Binding Energies (kcal/mol) of the FMA−Ac dimers A, B, and C at the MP2 Level of Theory

	MP2/aug-cc-pVDZ				MP2/cc-pVTZ			
	ΔE	BSSE	ZPE	$\Delta E_{(BSSE+ZPE)}$	ΔE	BSSE	ZPE	$\Delta E_{(BSSE+ZPE)}$
A	−5.59	1.32	1.27	−3.00	−5.20	1.10	1.14	−2.96
B	−4.84	1.16	1.12	−2.56	−4.62	1.06	1.10	−2.46
C	−3.67	1.10	0.80	−1.77	−3.12	0.59	0.74	−1.79

TABLE 2: Calculated Binding Energies (kcal/mol) of the FMA−Ac Trimers T-A to T-I at the MP2/aug-cc-pVDZ Level of Theory

	MP2/aug-cc-pVDZ			
	ΔE	BSSE	ZPE	$\Delta E_{(BSSE+ZPE)}$
T-A	−11.08	3.26	2.38	−5.44
T-B	−10.44	2.60	2.30	−5.54
T-C	−9.71	2.97	2.01	−4.73
T-D	−9.47	2.55	2.03	−4.89
T-E	−9.46	2.95	2.00	−4.51
T-F	−8.82	2.37	1.88	−4.57
T-G	−8.16	2.44	1.87	−3.85
T-H	−6.96	2.83	1.51	−2.62
T-I[a]	*−7.22*			

[a] T-**I** does not represent a minimum at this level of theory.

Computational Results

Dimers. Three FMA−Ac dimers were localized at the MP2 level of theory with the aug-cc-pVDZ and cc-pVTZ basis sets.

TABLE 3: Calculated and Experimental Vibrational Frequencies (cm^{-1}) of the FMA and Ac Monomers

MP2/cc-pVTZ	argon		nitrogen		
mode	calculated	experimental	factor of correction	experimental	factor of correction	assignment
			Formamide (FMA)			
6	1285.1	1260.4	0.981	1246.5	0.969	ν (C−N)
9	1811.0	1739.1	0.960	1736.1	0.958	ν (C═O)
10	3017.2	2882.9	0.955	2871.2	0.951	ν (C−H)
11	3634.7	3426.6	0.943	3430.5	0.943	ν_s (NH_2)
12	3787.1	3547.4	0.937	3553.2	0.938	ν_{as} (NH_2)
			Acetylene (Ac)			
5	753.0	736.8	0.978	742.1,747.6	0.988	δ (CCH)
3	3446.1	3288.8	0.954	3283.0	0.952	ν_{as} (C−H)

TABLE 4: Experimental and Calculated Vibrational Frequencies and Shifts (cm^{-1}) of the FMA−Acetylene Dimers A and B

		MP2/cc-pVTZ[a]						
argon matrix[a]	rel. int.	dimer **A** uncorrected	dimer **A** corrected[c]	rel. int.	dimer **B** uncorrected	dimer **B** corrected[c]	rel. int.	assingnment (mode)
			vibrational modes of the formamide fragment					
1273.1 (+12.7)	9	1304.0 (+18.9)	1279.2 (+18.5)	32	1299.7 (+14.6)	1275.0 (+14.3)	27	ν (C−N)(ν_6)
1276.9 (+16.5)	2							
1724.2 (−14.9)	30	1796.7 (−14.3)	1724.8 (−13.7)	99	1796.8 (−14.2)	1724.9 (−13.6)	100	ν (C═O)(ν_9)
1730.9 (−8.2)	100							
3399.1 (−27.5)	3	3603.6 (−31.1)	3398.2 (−29.3)	31	3631.9 (−2.8)	3424.9 (−2.6)	16	ν_s (NH_2)(ν_{11})
3536.2 (−11.2)	4	3767.9 (−19.2)	3530.5 (−18.0)	30	3783.7 (−3.4)	3545.3 (−3.2)	15	ν_{as} (NH_2)(ν_{12})
			vibrational modes of the acetylene fragment					
784.3 (+47.5)	7	812.4[b] (+59.4)	794.5[b] (+58.1)	22	815.5[b] (+62.5)	797.6[b] (+61.1)	16	δ(CCH)(ν_5)
790.4 (+53.6)	4							
795.7 (+58.9)	8	813.6 (+60.6)	795.7 (+59.3)	39	851.9 (+98.9)	833.2 (+96.7)	27	
819.3 (+82.5)	2							
3210.5 (−78.3)	21	3375.4 (−70.7)	3220.1 (−67.4)	60	3353.2 (−92.9)	3199.0 (−88.6)	77	ν_{as} (C−H)(ν_3)
3215.5 (−73.3)	13							
nitogen matrix[a]		MP2/cc-pVTZ[a]						
			vibrational modes of the formamide fragment					
1260.8 (+14.3)	20	1304 (+18.9)	1263.5 (+18.3)	32	1299.7 (+14.6)	1259.4 (+14.1)	27	ν (C−N)(ν_6)
1267.5 (+21.0)	2							
1726.0 (+10.1)	100	1796.7 (−14.3)	1721.2 (−13.7)	99	1796.8 (−14.2)	1721.3 (−13.6)	100	ν (C−O)(ν_9)
1729.3 (+6.8)	92							
3405.7 (−28.4)	5	3603.6 (−31.1)	3398.2 (−29.3)	31	3631.9 (−2.8)	3424.8 (−2.6)	16	ν_s (NH_2)(ν_{11})
3428.4 (−2.1)	14							
3540.7 (−12.5)	17	3767.9 (−19.2)	3534.3 (+18.0)	30	3783.7 (−3.4)	3550.0 (−3.2)	15	ν_{as} (NH_2)(ν_{12})
			vibrational modes of the acetylene fragment					
787.7(+43.4)	16	812.4[b] (+59.4)	802.6[b] (+58.7)	22	815.5[b] (+62.5)	805.7[b] (+61.7)	16	δ(CCH)(ν_5)
791.1 (+46.8)	18							
796.4 (+52.1)	10	813.6 (+60.6)	803.8 (+59.8)	39	851.9 (+98.9)	841.6 (+97.7)	27	
3221.4 (−61.6)	20							
3226.1 (−56.9)	50	3375. (−70.7)	3213.4 (−67.3)	60	3353.2 (−92.9)	3192.2 (−86.4)	77	ν_{as} (C−H)(ν_3)

[a] The frequency shifts in **A** compared to FMA and Ac (monomers M) are given in parentheses (Table 3). [b] Out of plane mode. [c] Correction factors see Table 3.

The geometries and ZPE+BSSE-corrected binding energies of the dimers are discussed here at the MP2/cc-pVTZ level of theory only, since there is a very good agreement between the calculated geometries and binding energies with both basis sets (Figure 11 and Table 1).

There are three basic interactions between the FMA and Ac molecules in the dimers:

(1) $N-H_{FMA}\cdots\pi$ interaction between the amide hydrogen atom of FMA and the π system of Ac.

(2) $C{=}O_{FMA}\cdots H_{acet}$ interaction between the carbonyl oxygen atom of FMA and one hydrogen atom of Ac.

(3) $C-H_{FMA}\cdots\pi$ interaction between the CH hydrogen atom of FMA and the π system of Ac.

The most stable dimer **A** (−2.96 kcal/mol) is stabilized by the $N-H_{FMA}\cdots\pi$ interaction (1) with distances of 2.447 and 2.973 Å to both carbon atoms of Ac. The $C{=}O_{FMA}\cdots H_{acet}$ interaction (2) at 2.216 Å additionally stabilizes dimer **A**, which is 0.50 kcal/mol more stable than complex **B** (−2.46 kcal/mol) (Figure 11 and Table 1).

In dimer **B**, interaction 2 shows a shorter hydrogen bond distance (2.114 Å) compared to that of dimer **A**. Complex **B** is additionally stabilized by a very weak $C-H_{FMA}\cdots\pi$ interaction (3) with 2.925 and 3.752 Å distance to both Ac carbon atoms. This shows the importance of the contribution of interaction 2 to the stabilization of both dimers **A** and **B**. In dimer **B**, albeit interaction 3 is very weak, it also contributes to define the shape of the complex. Dimer **C** is a very weakly interacting complex (−1.79 kcal/mol), which is only stabilized by interaction 1 with a $N-H_{FMA}\cdots C_{acet}$ distance of 2.490 Å to both Ac carbon atoms.

TABLE 5: Experimental and Calculated Vibrational Frequencies and Shifts (cm^{-1}) of the FMA−Ac 1:2 Complexes T-A and T-B

			MP2/Aug-cc-pVDZ[a]						
argon matrix[a]	rel. int.	**M**	trimer **A** uncorrected	trimer **A** corrected[c]	rel. int.	trimer **B** uncorrected	trimer **B** corrected[c]	rel. int.	assingnment (mode)
vibrational modes of the formamide fragment									
		1273.8	1299.6 (+25.8)	1285.5 (+25.5)	21	1305.7 (+31.9)	1291.3 (+31.5)	33	ν (C−N) (ν_6)
1722.3 (−16.8)	100	1763.3	1755.8 (−7.5)	1731.7 (−7.4)	100	1747.7 (−15.6)	1723.2 (−15.3)	99	ν (C═O) (ν_9)
		3604.4	3553.6 (−50.8)	3378.7 (−47.8)	48	3567.1 (−37.3)	3388.7 (−35.1)	36	ν_s (NH_2) (ν_{11})
		3763.6	3734.6 (−29.0)	3517.9 (−28.0)	23	3740.0 (−23.6)	3523.1 (−22.4)	29	ν_{as} (NH_2) (ν_{12})
vibrational modes of the acetylene fragment									
		703.2	758.2[b] (+55.0)	794.4[b] (+57.6)	12	753.2[b] (+50.0)	788.6[b] (+52.3)	31	δ(CCH) (ν_5)
			768.8[b] (+65.6)	804.9[b] (+68.7)	20	763.7[b] (+60.5)	799.6[b] (+63.3)	18	
			805.0 (+101.5)	842.8 (+106.2)	20	776.8 (+73.6)	813.3 (+77.1)	23	
			805.3 (+102.3)	843.1 (+107.1)	20	800.5 (+97.3)	838.1 (+101.8)	32	
3198.4 (−90.4)	15	3431.4	3342.9 (−89.0)	3202.5 (−85.2)	75	3339.6 (−91.8)	3199.3 (−87.9)	99	ν_{as} (C−H) (ν_3)
3232.2 (−56.6)	10		3381.1 (−50.3)	3239.1 (−48.1)	65	3374.9 (−56.5)	3233.1 (−54.1)	40	
nitrogen matrix[a]									
vibrational modes of the formamide fragment									
1274.9 (+28.3)	15	1273.8	1299.6 (+25.8)	1271.7 (+25.2)	21	1305.7 (+31.9)	1276.9 (+31.4)	33	ν (C−N) (ν_6)
1721.9 (−14.2)	100	1763.3	1755.8 (−7.5)	1728.7 (−7.4)	100	1747.7 (−15.6)	1719.7 (−15.3)	99	ν (C═O) (ν_9)
−		3604.4	3553.6 (−50.8)	3382.1 (−47.9)	48	3567.1 (−37.3)	3392.3 (−35.2)	36	ν_s (NH_2) (ν_{11})
−		3763.6	3734.6 (−29.0)	3525.8 (−27.6)	23	3740.0 (−23.6)	3530.5 (−22.4)	29	ν_{as} (NH_2) (ν_{12})
vibrational modes of the acetylene fragment									
−		703.2	758.2[b] (+55.0)	802.2[b] (+58.2)	12	753.2[b] (+50.0)	796.8[b] (+52.9)	31	δ(CCH) (ν_5)
−			768.8[b] (+65.6)	813.4[b] (+69.4)	20	763.7[b] (+60.5)	807.9[b] (+64.0)	18	
−			805.0 (+101.5)	851.7 (+107.4)	20	776.8 (+73.6)	821.8 (+77.8)	23	
−			805.3 (+102.3)	852.0 (+108.2)	20	800.5 (+97.3)	846.9 (+102.9)	32	
3215.5 (67.5)	15	3431.4	3342.9 (−89.0)	3195.8 (−85.1)	75	3339.6 (−91.8)	3192.6 (−87.7)	99	ν_{as} (C−H) (ν_3)
	10		3381.1 (−50.3)	3232.3 (−48.1)	65	3374.9 (−56.5)	3226.4 (−54.0)	40	

[a] The frequency shifts in trimers T-**A** and T-**B** compared to FMA and acetylene monomers. [b] Out of plane mode. [c] Factors of correction for the MP2/aug-cc-pVDZ level of theory (argon): FMA C−N stretching: 0.989; C═O stretching: 0.986; $N-H_{sym}$ stretching: 0.942; $N-H_{as}$ stretching: 0.95. Ac C−H bending: 1.047; C−H stretching: 0.958. [d] Factors of correction for the MP2/aug-cc-pVDZ level of theory (nitrogen): FMA C−N stretching: 0.978; C═O stretching: 0.984; $N-H_{sym}$ stretching: 0.944, $N-H_{as}$ stretching: 0.951. Ac C−H bending: 1.058; C−H stretching: 0.956.

Trimers. Eight 1:2 FMA−Ac trimers (T-**A** to T-**H**) were localized at the MP2/aug-cc-pVDZ level of theory, using the MMH approach and starting from 200 randomly generated geometries. (Figure 12) Complex T-**I** is not a minimum at this level of theory, since it shows one imaginary frequency (−11.24 cm^{-1}) of Ac2, distorting the Cs symmetry of the complex. Despite this, T-**I** is presented here because of its similarity to trimer T-**H** and the fact that they are both stabilized exclusively by H···π interactions.

Similarly to the dimers, the 1:2 FMA−Ac complexes are stabilized by interactions 1, 2, and 3, but there is also the $C-H_{acet}$···π interaction (interaction 4) between both molecules of Ac. Trimers T-**A** and T-**B** are the most stable complexes

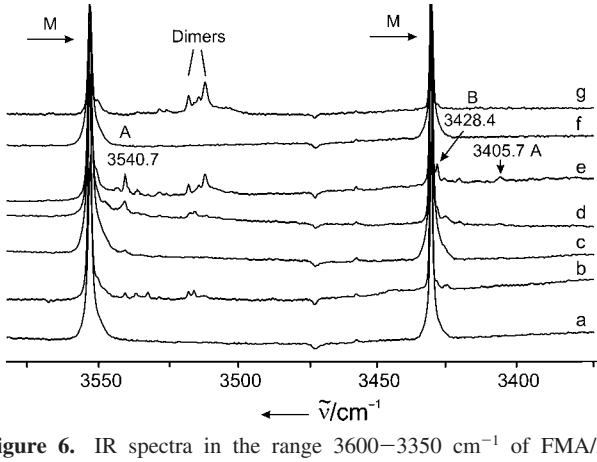

Figure 6. IR spectra in the range 3600−3350 cm^{-1} of FMA/Ac mixtures matrix-isolated in nitrogen: (a) FMA/Ac/N_2 ratio 1:1:600, 10 K; (b) FMA/Ac/N_2 ratio 1:1:600, after annealing at 30 K; (c) FMA/Ac/N_2 ratio 1:3:600, 10 K; (d) FMA/Ac/N_2 ratio 1:3:600 after annealing at 25 K; (e) FMA/Ac/N_2 ratio 1:3:600 after annealing at 30 K; (f) FMA/N_2 ratio 1:600, 10 K; (g) FMA/N_2 ratio 1:600, after annealing at 25 K.

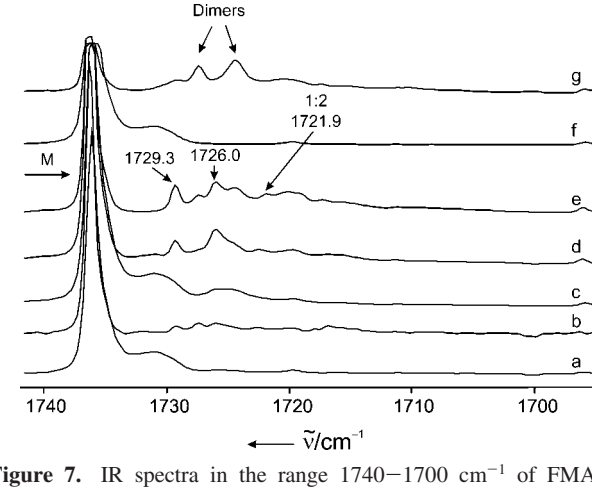

Figure 7. IR spectra in the range 1740−1700 cm^{-1} of FMA/Ac mixtures matrix-isolated in nitrogen: (a) FMA/Ac/N_2 ratio 1:1:600, 10 K; (b) FMA/Ac/N_2 ratio 1:1:600, after annealing at 30 K; (c) FMA/Ac/N_2 ratio 1:3:600, 10 K; (d) FMA/Ac/N_2 ratio 1:3:600 after annealing at 25 K; (e) FMA/Ac/N_2 ratio 1:3:600 after annealing at 30 K; (f) FMA/N_2 ratio 1:600, 10 K; (g) FMA/N_2 ratio 1:600, after annealing at 25 K.

TABLE 6: Calculated (MP2/cc-pVTZ) Vibrational Frequencies (cm^{-1}) of the FMA−Ac Dimer C

dimer **C** without correction		corrected argon		corrected nitrogen		relative intensity	assignment
			Formamide (FMA)[a]				
1288.4	(+3.3)	1263.9	(+3.2)	1248.4.	(+1.9)	25	ν (C−N) (ν_6)
1806.5	(−4.5)	1734.2	(−4.3)	1730.6	(−5.5)	99	ν (C═O) (ν_9)
3608.2	(−0.6)	2880.8	(−0.57)	2868.8	(−2.4)	21	ν (C−H) (ν_{10})
3608.2	(−26.5)	3402.5	(−25.0)	3402.5	(−25.0)	33	ν_s (NH_2) (ν_{11})
3759.7	(−27.4)	3522.8	(−25.7)	3526.5	(−26.7)	40	ν_{as} (NH_2) (ν_{12})
			Acetylene (Ac)[a]				
756.1[b]	(+3.1)	739.5[b]	(+3.0)	747.0[b]	(+2.7)	21	δ (CCH) (ν_5)
762.5	(+9.5)	745.7	(+9.3)	753.3	(+9.5)	26	
3436.0	(−10.1)	3277.9	(−9.6)	3271.1	(−11.9)	29	ν_{as} (C−H)) (ν_3)

[a] The frequency shifts in **C** compared to FMA and Ac (monomers M) are given in parentheses (Table 3). [b] Out of plane mode.

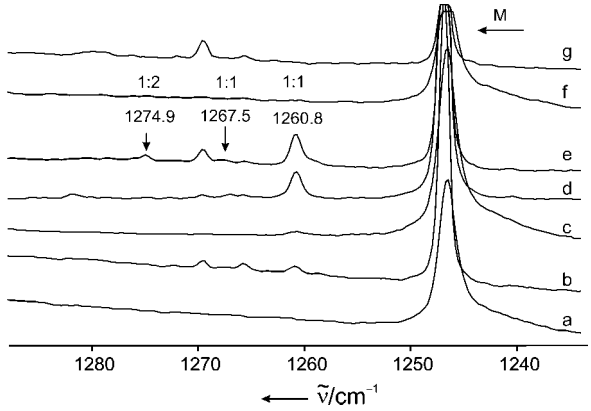

Figure 8. IR spectra in the range 1280−1240 cm^{-1} of FMA/Ac mixtures matrix-isolated in nitrogen: (a) FMA/Ac/N_2 ratio 1:1:600, 10 K; (b) FMA/Ac/N_2 ratio 1:1:600, after annealing at 30 K; (c) FMA/Ac/N_2 ratio 1:3:600, 10 K; (d) FMA/Ac/N_2 ratio 1:3:600 after annealing at 25 K; (e) FMA/Ac/N_2 ratio 1:3:600 after annealing at 30 K; (f) FMA/N_2 ratio 1:600, 10 K; (g) FMA/N_2 ratio 1:600, after annealing at 25 K.

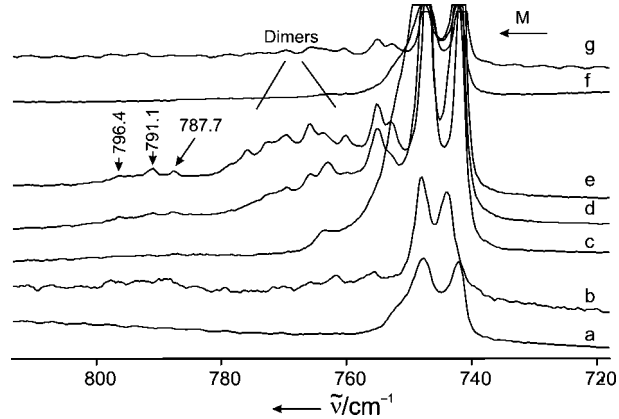

Figure 10. IR spectra in the range 810−720 cm^{-1} of FMA/Ac mixtures matrix-isolated in nitrogen: (a) FMA/Ac/N_2 ratio 1:1:600, 10 K; (b) FMA/Ac/N_2 ratio 1:1:600, after annealing at 30 K; (c) FMA/Ac/N_2 ratio 1:3:600, 10 K; (d) FMA/Ac/N_2 ratio 1:3:600 after annealing at 25 K; (e) FMA/Ac/N_2 ratio 1:3:600 after annealing at 30 K; (f) FMA/N_2 ratio 1:600, 10 K; (g) FMA/N_2 ratio 1:600, after annealing at 25 K.

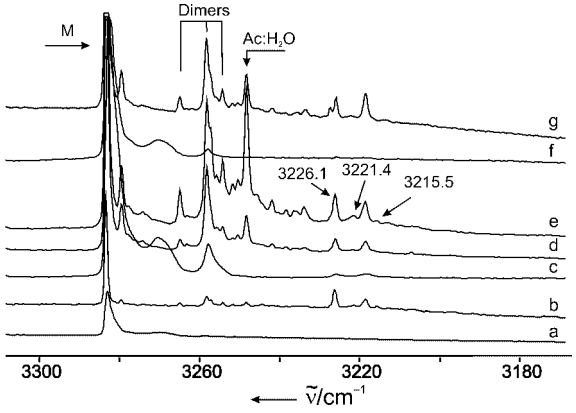

Figure 9. IR spectra in the range 3300−3200 cm^{-1} of FMA/Ac mixtures matrix-isolated in nitrogen: (a) FMA/Ac/N_2 ratio 1:1:600, 10 K; (b) FMA/Ac/N_2 ratio 1:1:600, after annealing at 30 K; (c) FMA/Ac/N_2 ratio 1:3:600, 10 K; (d) FMA/Ac/N_2 ratio 1:3:600 after annealing at 25 K; (e) FMA/Ac/N_2 ratio 1:3:600 after annealing at 30 K; (f) FMA/N_2 ratio 1:600, 10 K; (g) FMA/N_2 ratio 1:600, after annealing at 25 K.

and, with −5.44 and −5.54 kcal/mol, respectively, are very close in energy (for the trimers, all energies discussed here are at the MP2/aug-cc-pVDZ + BSSE + ZPE level of theory, Table 2). The trimer T-**A** is stabilized by the N−H_{FMA}···π interaction (1) of FMA with the first Ac molecule Ac1, the C═O_{FMA}···H_{acet} interaction (2) FMA−Ac2, and the C−H_{acet}···π interaction (4) between both molecules of Ac resembling the well established "T"-shaped Ac dimer.[42−49]

In complex T-**B**, the two molecules of Ac do no interact with each other. Instead, the oxygen atom of FMA interacts with the hydrogen atoms of both molecules of Ac (interaction 2), and one of the FMA N−H hydrogen atoms interacts with the π system of Ac1 (interaction 1). The position of Ac2 with respect to the FMA molecule indicates a very weak C−H···π interaction (3), which also has been found in the 1:2 formic acid (FA)−Ac trimers.[17]

At this point, it is very interesting to compare the geometries of the 1:2 FMA−Ac T-**A** and T-**B** trimers with the two most stable 1:2 FA−Ac complexes (F-**A** and F-**B**) previously studied in our group (Figure 13).[17] It is remarkable that, starting from completely randomly generated geometries without any previous chemical assumptions, the 1:2 FMA and the FA complexes with Ac show very similar structures. The 1:2 FA−Ac trimer F-**A** is stabilized by the O−H_{FA}···π interaction involving one molecule of Ac, and the C═O_{FA}···H_{acet} interaction involving the second molecule of Ac, together with the Ac−Ac C−H_{acet}···π "T" interaction, similarly to the 1:2 FMA−Ac complex T-**A**.

Similar to the 1:2 FMA−Ac complex T-**B**, the FA−Ac trimer F-**B** also does not show any interaction between the two molecules of Ac. F-**B** is stabilized by the O−H_{FA}···π interaction with Ac1 and C═O_{FA}···H_{acet} interactions with both molecules of Ac. In both T-**B** and F-**B**, the second molecule of Ac stabilizes the trimer via a C−$H_{FA(FMA)}$···π interaction.

1:2 FMA−Ac trimers T-**C** and T-**D** are very close in energy as well (−4.73 and −4.89 kcal/mol, respectively), and both are stabilized by interactions 1 and 2. The difference is that, in trimer

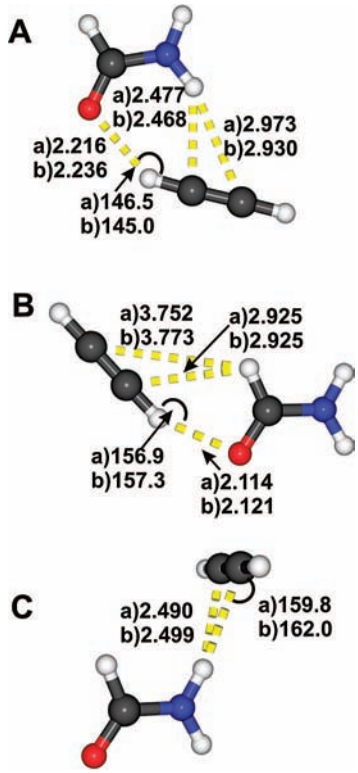

Figure 11. The calculated structures with hydrogen bond lengths (Å) of the FMA−Ac dimers **A**, **B**, and **C** at the (a) MP2/cc-pVTZ and (b) MP2/aug-cc-pVDZ levels of theory.

T-**C**, interaction 1 involves only the π system of Ac2, while, in T-**D**, both amide hydrogen atoms of FMA are involved in $N-H_{FMA}\cdots\pi$ interactions with Ac1 and Ac2. In addition, in trimer T-**C**, the two molecules of Ac form a "T" dimer in a plane almost parallel to FMA. Therefore, unlike trimer T-**D**, complex T-**C** is stabilized also by the $C-H_{acet}\cdots\pi$ interaction (4) (Figure 13).

The difference between the corrected binding energies of trimers T-**E** (−4.51 kcal/mol) and T-**F** (−4.57 kcal/mol) is only 0.06 kcal/mol. Both complexes show interaction 2 between the carbonyl oxygen atom of FMA and Ac1 and the $C-H_{FMA}\cdots\pi$ interaction (3). In the case of T-**F**, interaction 3 is between FMA and Ac1, whereas, in T-**E**, the C−H hydrogen atom of FMA weakly interacts with the π system of Ac2. T-**E** is also stabilized by interaction 4 between both molecules of Ac forming the "T" dimer, while trimer T-**F** lacks the $C-H_{acet}\cdots\pi$ interaction (4).

In trimer T-**G** (−3.85 kcal/mol), the interactions between FMA and Ac1 resemble the structure of the FMA−Ac dimer **A** (Figures 11 and 12). Complex T-**G** is additionally stabilized by the $C-H_{acet}\cdots\pi$ interaction (4) between both molecules of Ac.

T-**H** (−2.62 kcal/mol) and T-**I** are very interesting structures, since they are only stabilized by the $N-H\cdots\pi$ and $C-H\cdots\pi$ interactions. As already mentioned, T-**I** is not a minimum at this level of theory. In complex T-**H**, Ac1 lies in the same plane as FMA and shows a $C-H\cdots\pi$ interaction, whereas Ac2 is perpendicular to FMA and shows a $N-H\cdots\pi$ interaction. The subunit formed by the FMA molecule and Ac2 reproduces the geometry of the FMA−Ac dimer **C** (Figures 11 and 12).

In the trimer T-**I**, Ac1 lies in a perpendicular plane relative to FMA and Ac2 in the same plane. The explanation why T-**I** is a transition state can be found by comparing the subunits formed by the Ac molecule perpendicular to FMA and the FMA molecule. In trimer T-**H**, this subunit (FMA−Ac2) resembles

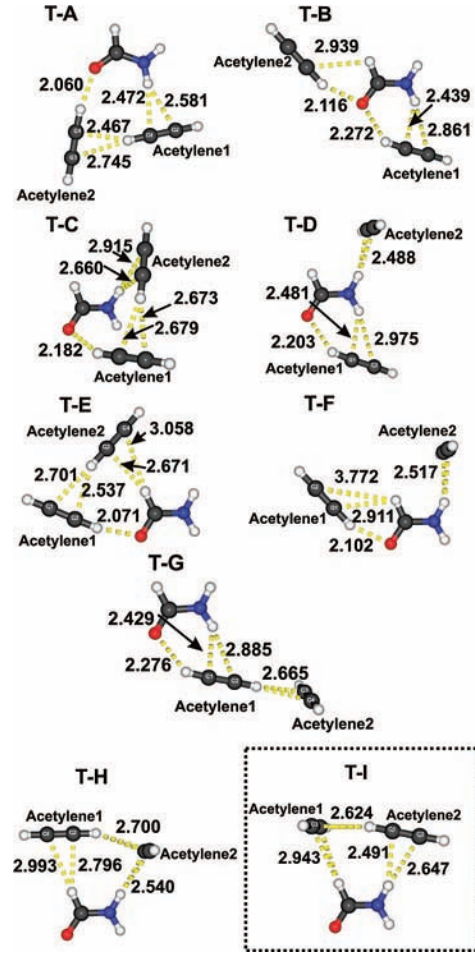

Figure 12. The calculated structures with hydrogen bond lengths (Å) of the FMA−Ac trimers T-**A** to T-**I** at the MP2/aug-cc-pVDZ level of theory.

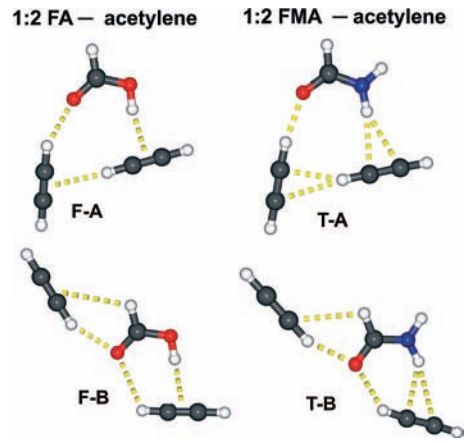

Figure 13. FMA−Ac trimers T-**A** and T-**B** and FA−Ac trimers F-**A** and F-**B** at the MP2/cc-pVTZ level of theory.

the geometry of FMA−Ac dimer **C**, whereas, in trimer T-**I**, the FMA−Ac1 subunit is only stabilized by the very weak $C-H_{FMA}\cdots\pi$ interaction.

Comparison of Calculated and Experimental Vibrational Frequencies: Dimers A and B. The experimental vibrational frequencies of the FMA−Ac dimers were compared to MP2/cc-pVTZ calculations (Tables 4−6). The deviations between the experimental and calculated modes are attributed to matrix shifts as well as deficiencies of the theoretical model (e.g., not considering the anharmonicity of the vibrations). Scaling factors

for each vibrational mode of the FMA and Ac monomers were calculated to correct for these deviations. These scaling factors, by definition, exactly reproduce the experimental values of the monomers (Table 3). Applying the scaling factor to the modes of the complexes allows one to reliably predict the band positions of the complexes.

N−H and Acetylene C−H Stretching Vibrations. Our experimental data in argon and nitrogen matrices indicate the formation of two cyclic FMA−Ac complexes **A** and **B**. In the N−H stretching region in argon, new bands at 3399.1 (−27.5) and 3536.2 (−11.2) cm^{-1} are observed, in good agreement with the predictions from the MP2/cc-pVTZ calculations for complex **A** (scaled, Table 4). In nitrogen, a similar agreement between experiment and calculation was found. In dimer **B**, the NH group of FMA is not engaged in hydrogen bonding (Figure 11), and thus the NH stretching vibration of the FMA subunit in **B** shows only small shifts compared to the FMA monomer band. In argon, the shift was too small to be detected, whereas, in nitrogen, a new band at 3428.4 cm^{-1} (red shift −2.1 cm^{-1}) is assigned to the symmetric stretching vibration mode of FMA in dimer **B**.

The large shifts in the C−H stretching and bending modes of Ac show that the Ac hydrogen atoms are the hydrogen bond donors. The shift of the $\nu 3$ mode of Ac is a good indicator of the hydrogen bond strength.[50,51] According to our calculations, the largest shifts are expected for the C−H stretching vibration of Ac in complex **A**, which, after scaling, is predicted at 3220.1 cm^{-1} and 3213.4 cm^{-1} in argon and nitrogen, respectively (Table 4, the difference is due to different scaling factors in argon and nitrogen). For dimer **B**, the C−H stretching vibration is calculated to 3199.0 cm^{-1} (argon, Figure 4, Table 4). The C−H stretching vibration calculated for complex **A** at 3220.1 cm^{-1} (argon) agrees well with both experimentally observed bands at 3215.5 and 3210.5 cm^{-1}. The difference between the experimental bands (3215.5 and 3210.5 cm^{-1}) is only 5 cm^{-1} (calculated 21.1 cm^{-1}). Although it is clear that two complexes are formed, the small differences do not allow a reliable assignment of the C−H stretching vibrations to dimer **A** or **B**.

The C−H stretching vibration of monomeric Ac in a nitrogen matrix is found at 3283.0 cm^{-1} together with a weak doublet at 3227.4 and 3225.7 cm^{-1} (Figure 9). A singlet at 3218.5 cm^{-1} is assigned to the well-known Ac−water complex.[41] In the presence of both FMA and Ac, an additional band at 3226.1 cm^{-1} is found. For dimer **A**, the calculations (MP2/cc-pVTZ) predict this band at 3213.4 cm^{-1} (red-shifted by 67.3 cm^{-1} from the monomer), quite close to the experimental value (Table 4). For dimer **B**, this band is expected at 3192.2 cm^{-1} (red-shifted by 86.4 $cm^{-1}$from the monomer) in less agreement with the experiment.

Acetylene C−H Bending Vibrations. An additional criterion for the hydrogen bond formation in Ac complexes is the blue shift of the C−H bending modes of the Ac unit. The C−H bending modes in complex **A** are predicted (MP2/cc-pVTZ, scaled) at 795.7 (+59.3) and 794.5 (+58.1) cm^{-1} in argon and at 803.8 (+59.8) and 802.6 (+58.7) cm^{-1} in nitrogen, respectively, thus showing the expected blue shifts (Table 4). For complex **B**, bands are predicted at 833.2 (+96.7) and 797.6 (+61.1) cm^{-1}in argon and at 841.6 (+97.7) and 805.7 (+61.7) cm^{-1}in nitrogen. The band observed at 819.3 cm^{-1} in argon with the large blue shift of +82.5 cm^{-1} is thus assigned to complex **B**, whereas the other three bands at 795.7 (+58.9), 790.4 (+53.6), and 784.3 (+47.5) cm^{-1} could either belong to **A** or **B** (Figure 5). In nitrogen, only three bands at 796.4, 791.1, and 787.7 cm^{-1} are observed.

C═O Stretching Vibrations. The presence of two shifted C═O stretching vibrations at 1730.9 and 1724.2 cm^{-1} in argon and at 1729.3 and 1726.0 cm^{-1} in nitrogen indicates that two complexes are formed, with the carbonyl group as the hydrogen bond acceptor. For complexes **A** and **B**, the C═O stretching vibrations are calculated (scaled) to 1724.8 and 1724.9 cm^{-1}, respectively, in argon, and 1721.2 cm^{-1} and 1721.3 cm^{-1}, respectively, in nitrogen (Table 4). Since the C═O stretching vibrations in both complexes are very close, a definitive assignment was not possible.

C−N Stretching Vibrations. The formation of FMA−Ac complexes results in blue shifts of the C−N stretching vibrations (Figures 3 and 8). In argon, a weak band at 1276.9 and a strong band at 1273.1 cm^{-1} are assigned to FMA−Ac complexes. In nitrogen, new bands in this region are observed at 1274.9 (probably more than one Ac molecule involved), 1267.5, and 1260.8 cm^{-1}.

The C−N stretching mode of **A** is calculated (MP2/cc-pVTZ, scaled) at 1279.2 cm^{-1} in argon and 1263.5 cm^{-1} in nitrogen, and that of **B** is calculated at 1275.0 cm^{-1} in argon and 1259.4 cm^{-1} in nitrogen, respectively. We therefore assign the bands at higher frequency to dimer **A** and that at lower frequency to dimer **B**.

The comparison between our calculated and experimental spectra shows that we are able to trap both dimer **A** and **B** in argon and nitrogen matrices, whereas complex **C** is not observed. Since the expected shifts for many bands in **A** and **B** are small or very similar, the assignments can only be tentative in these cases.

Comparison of Calculated and Experimental Vibrational Frequencies: Trimers. At higher concentrations of Ac in the matrix experiments, new peaks appear in the spectra that cannot be assigned to the monomers or to the dimers. The intensities of these absorptions increase with the Ac concentration, indicating that more than one molecule of Ac is involved. In argon, the weak absorption at 1722.3 cm^{-1} is assigned to the carbonyl stretching mode of FMA in the T-**B** trimer (Table 5). In nitrogen, the absorption at 1721.9 cm^{-1} is assigned to the carbonyl stretching vibration of FMA in the trimer T-**B**. The experimentally observed shift of the C═O stretching vibration (−16.8 cm^{-1} in argon and −14.2 cm^{-1} in nitrogen) is in good agreement with the shift calculated for trimer T-**B** (−15.3 cm^{-1} in argon and nitrogen), while that calculated for trimer T-**A** is smaller (−7.4 cm^{-1} in argon and nitrogen). However, because of the small difference, this assignment is only tentative.

Other weak absorptions that could be assigned to trimers are found in the C−H stretching region of Ac: 3232.2 (−56.6) and 3198.4 (−90.4) cm^{-1} in argon and 3215.5 (−67.5 cm^{-1}) in nitrogen (Figure 4, Table 6). These bands are in good agreement with the calculated values for both trimers T-**A** and T-**B** (−48.1 and −85.2 cm^{-1} for T-**A** and −54.1 and −87.9 cm^{-1} for T-**B**, respectively). In the nitrogen matrix, a new band at 1274.9 cm^{-1} is found at high concentration of Ac, which is close to the calculated values for both trimers T-**A** and T-**B** (Figure 8). The IR data indicate that trimers with two molecules of Ac are formed at high concentrations of Ac. However, on the basis of these data, an assignment to one of the most stable trimers T-**A** and T-**B** is not possible.

Conclusions

Using matrix isolation techniques and ab initio calculations, we found that two FMA−Ac dimers are formed in the matrix. In addition, there is evidence for the formation of an FMA−Ac trimer at higher concentrations of Ac. Three stable FMA−Ac

dimers were predicted by calculations at the MP2 level of theory with the aug-cc-pVDZ and cc-pVTZ basis sets. Their binding energies are between −2.96 and −1.79 kcal/mol (MP2/cc-pVTZ +ZPE+BSSE). The most stable dimer **A** is stabilized by the $N-H_{FMA}\cdots\pi$ and $C{=}O_{FMA}\cdots H_{acet}$ interactions between FMA and Ac. Dimer **B** shows the $C-H_{FMA}\cdots\pi$ and $C{=}O_{FMA}\cdots H_{acet}$ interactions, while dimer **C** is stabilized only by the $N-H_{FMA}\cdots\pi$ interactions. By comparing the experimental and calculated frequencies, dimers **A** and **B** were identified in argon and nitrogen matrices. Both complexes are dominated by the strong $C{=}O_{FMA}\cdots H_{acet}$ interactions, which results in large shifts of the Ac C−H stretching modes.

It is interesting to compare the structures of **A** and **B** to the most stable dimers between FA and Ac.[21] The most stable dimers **A** both show a $C{=}O\cdots H_{acet}$ interaction and an $X-H\cdots\pi$ interaction (X = N and O, respectively). However, because of its higher acidity, FA forms a strong and short (2.216 Å at the MP2/aug-cc-pVTZ level of theory) $O-H\cdots\pi$ interaction with the Ac molecule, which dominates the structure of the dimer (the O−H bond points in an almost right angle toward the center of the Ac π-bond).[21] In the FMA−ac complex **A**, the corresponding $N-H\cdots\pi$ distance is 2.973 Å (calculated at the MP2/cc-pVTZ level of theory) and is therefore much longer. On the other hand, the $C{=}O\cdots H_{acet}$ interaction in the FA−Ac dimer **A** is much longer than that in the FMA−Ac dimer **A**. Thus, with FA, the $O-H\cdots\pi$ interaction dominates the structure, while with FMA the $C{=}O\cdots H_{acet}$ interaction is dominant, which reveals that the capability of the X−H hydrogen atom to act as a hydrogen bond donor modulates the structure of the complexes. This becomes clear by comparing the second most stable complexes **B** for both FMA−Ac and FA−Ac, which do not involve the X−H hydrogen atom and which are very similar in structure.

Eight 1:2 FMA−Ac trimers (T-**A** to T-**H**) with binding energies between −5.44 and −2.62 kcal/mol were identified by calculations (MP2/aug-cc-pVDZ + ZPE +BSSE). The trimers T-**A** and T-**B** are close in energy. Weak bands observed under matrix isolation conditions at higher concentrations of Ac suggest the formation of trimers. However, the spectra calculated for the most stable trimers are too similar to allow for a clear assignment to either trimer T-**B** or T-**A**. The structural similarity between the most stable trimers in the system FMA−Ac and FA−Ac (Figure 13) is much larger than that of the corresponding dimers. This can be rationalized by the larger flexibility of complexes with two molecules of Ac, which more easily are able to adopt geometries that are both optimal for strong $X-H\cdots\pi$ and $C{=}O\cdots H_{acet}$ interactions.

Acknowledgment. This work was financially supported by the Deutsche Forschungsgemeinschaft (Forschergruppe 618), the European Commission in the framework of the project INTCHEM (MEST-CT-2005-020681), and the Fonds der Chemischen Industrie.

References and Notes

(1) Homer, R. B.; Johnson, C. D. *Chem. Amides* **1970**, 187–243.
(2) Sigel, H.; Martin, R. B. *Chem. Rev.* **1982**, *82*, 385–426.
(3) Räsänen, M. *J. Mol. Struct.* **1983**, *101*, 275–286.
(4) Räsänen, M. *J. Mol. Struct.* **1983**, *102*, 235–242.
(5) Engdahl, A.; Nelander, B.; Aastrand, P. O. *J. Chem. Phys.* **1993**, *99*, 4894–4907.
(6) Bohn, R. B.; Andrews, L. *J. Phys. Chem.* **1989**, *93*, 5684–5692.
(7) Schultz, P. W.; Leroi, G. E.; Popov, A. I. *J. Am. Chem. Soc.* **1995**, *117*, 10735–10742.
(8) Lundell, J.; Krajewska, M.; Raesaenen, M. *J. Phys. Chem. A* **1998**, *102*, 6643–6650.
(9) Maier, G.; Endres, J. *Eur. J. Org. Chem.* **2000**, *106*, 1–1063.
(10) Sundararajan, K.; Vidya, V.; Sankaran, K.; Viswanathan, K. S. *Spectrochim. Acta A* **2000**, *56A*, 1855–1867.
(11) Hartmann, M.; Wetmore, S. D.; Radom, L. *J. Phys. Chem. A* **2001**, *105*, 4470–4479.
(12) Tsuzuki, S.; Honda, K.; Uchimaru, T.; Mikami, M.; Tanabe, K. *J. Am. Chem. Soc.* **2000**, *122*, 3746–3753.
(13) Jeng, M. L. H.; DeLaat, A. M.; Ault, B. S. *J. Phys. Chem.* **1989**, *93*, 3997–4000.
(14) DeLaat, A. M.; Ault, B. S. *J. Am. Chem. Soc.* **1987**, *109*, 4232–4236.
(15) Jeng, M. L. H.; Ault, B. S. *J. Phys. Chem.* **1990**, *94*, 4851–4855.
(16) Sanchez-Garcia, E.; Studentkowski, M.; Montero, L. A.; Sander, W. *ChemPhysChem* **2005**, *6*, 618–624.
(17) Sanchez-Garcia, E.; George, L.; Montero, L. A.; Sander, W. *J. Phys. Chem. A* **2004**, *108*, 11846–11854.
(18) Montero, L. A.; Molina, J.; Fabian, J. *Int. J. Quantum Chem.* **2000**, *79*, 8–16.
(19) Montero, L. A.; Esteva, A. M.; Molina, J.; Zapardiel, A.; Hernandez, L.; Marquez, H.; Acosta, A. *J. Am. Chem. Soc.* **1998**, *120*, 12023–12033.
(20) Sanchez-Garcia, E.; Montero, L. A.; Sander, W. *J. Phys. Chem. A* **2006**, *110*, 12613−12622.
(21) George, L.; Sanchez-Garcia, E.; Sander, W. *J. Phys. Chem. A* **2003**, *107*, 6850–6858.
(22) Dewar, M. J. S.; Zoebisch, E. G.; Healy, E. F.; Stewart, J. J. P. *J. Am. Chem. Soc.* **1985**, *107*, 3902–3909.
(23) Stewart, J. J. P. *MOPAC v 6.0*.
(24) Stewart, J. J. P. *J. Comput. Chem.* **1989**, *10*, 209–264.
(25) Stewart, J. J. P. *J. Comput.-Aided Mol. Des.* **1990**, *4*, 1–105.
(26) Moller, C.; Plesset, M. S. *Phys. Rev.* **1934**, *46*, 618–622.
(27) Krishnan, R.; Binkley, J. S.; Seeger, R.; Pople, J. A. *J. Chem. Phys.* **1980**, *72*, 650–654.
(28) Frisch, M. J.; Pople, J. A.; Binkley, J. S. *J. Chem. Phys.* **1984**, *80*, 3265–3269.
(29) Dunning, T. H. Jr. *J. Chem. Phys.* **1989**, *90*, 1007–1023.
(30) Frisch, M. J.; Trucks, G. W.; Schlegel, H. B.; Scuseria, G. E.; Robb, M. A.; Cheeseman, J. R.; Zakrzewski, V. G.; Montgomery, J. A. Jr.; Stratmann, R. E.; Burant, J. C.; Dapprich, S.; Millam, J. M.; Daniels, A. D.; Kudin, K. N.; Strain, M. C.; Farkas, O.; Tomasi, J.; Barone, V.; Cossi, M.; Cammi, R.; Mennucci, B.; Pomelli, C.; Adamo, C.; Clifford, S.; Ochterski, J.; Petersson, G. A.; Ayala, P. Y.; Cui, Q.; Morokuma, K.; Malick, D. K.; Rabuck, A. D.; Raghavachari, K.; Foresman, J. B.; Cioslowski, J.; Ortiz, J. V.; Stefanov, B. B.; Liu, G.; Liashenko, A.; Piskorz, P.; Komaromi, I.; Gomperts, R.; Martin, R. L.; Fox, D. J.; Keith, T.; Al-Laham, M. A.; Peng, C. Y.; Nanayakkara, A.; Gonzalez, C.; Challacombe, M.; Gill, P. M. W.; Johnson, B. ; Chen, W.; Wong, M. W.; Andres, J. L.; Head-Gordon, M.; Replogle, E. S.; Pople, J. A. *Gaussian 98, Revision A.3*; Gaussian, Inc.: Pittsburgh PA, 1998.
(31) Frisch, M. J.; Schlegel, G. W. T. H. B.; Scuseria, G. E.; Robb, M. A.; Montgomery, J. R. C. J. A.; Vreven, Jr. T.; Kudin, K. N.; Millam, J. C. B. J. M; Iyengar, S. S.; Tomasi, J.; Barone, V.; Cossi, B. M. M.; Scalmani, G.; Rega, N.; Petersson, G. A.; Hada, H. N. M.; Ehara, M.; Toyota, K.; Fukuda, R.; Ishida, J. H. M.; Nakajima, T.; Honda, Y.; Kitao, O.; Nakai, H.; Knox, M. K. X. Li. J. E; Hratchian, H. P.; Cross, J. B.; Adamo, C.; Gomperts, J. J. R.; Stratmann, R.; Yazyev, O.; Austin, A. J.; Pomelli, R. C. C.; Ochterski, J. W.; Ayala, P. Y.; Morokuma, K.; Salvador, G. A. V. P.; Dannenberg, J. J.; Zakrzewski, V. G.; Daniels, S. D. A. D.; Strain, M. C.; Farkas, O.; Rabuck, D. K. M. A. D.; Raghavachari, K.; Foresman, J. B.; Cui, J. V. O. Q.; Baboul, A. G.; Clifford, S.; Cioslowski, J.; Liu, B. B. S. G.; Liashenko, A.; Piskorz, P.; Komaromi, I.; Fox, R. L. M. D. J.; Keith, T.; Al-Laham, M. A.; Peng, C. Y.; Challacombe A. N. M., Gill, P. M. W.; Johnson, B.; Wong, W. C. M. W.; Gonzalez, C.; Pople, J. A. *Gaussian 03, Revision B.03*; Gaussian, Inc.: Pittsburgh PA, 2003.
(32) Boys, S. F.; Bernardi, F. *Mol. Phys.* **1970**, *19*, 553.
(33) King, S.-T. *J. Phys. Chem.* **1971**, *75*, 405–410.
(34) Kline, E. S.; Kafafi, Z. H.; Hauge, R. H.; Margrave, J. L. *J. Am. Chem. Soc.* **1985**, *107*, 7559–7562.
(35) McDonald, S. A.; Johnson, G. L.; Keelan, B. W.; Andrews, L. *J. Am. Chem. Soc.* **1980**, *102*, 2892–2896.
(36) Jovan Jose, K. V.; Gadre Shridhar, R.; Sundararajan, K.; Viswanathan, K. S. *J. Chem. Phys.* **2007**, *127*, 104501.
(37) Jemmis, E. D.; Giju, K. T.; Sundararajan, K.; Sankaran, K.; Vidya, V.; Viswanathan, K. S.; Leszczynski, J. *J. Mol. Struct.* **1999**, *510*, 59–68.
(38) Sundararajan, K.; Sankaran, K.; Viswanathan, K. S.; Kulkarni, A. D.; Gadre, S. R. *J. Phys. Chem. A* **2002**, *106*, 1504–1510.
(39) Mardyukov, A.; Sanchez-Garcia, E.; Rodziewicz, P.; Doltsinis, N. L.; Sander, W. *J. Phys. Chem. A* **2007**, *111*, 10552–10561.
(40) Engdahl, A.; Nelander, B. *Chem. Phys. Lett.* **1983**, *100*, 129–132.
(41) Sundararajan, K.; Viswanathan, K. S. *J. Mol. Struct.* **2006**, *798*, 109–116.

(42) Karpfen, A. *J. Phys. Chem. A* **1999**, *103*, 11431–11441.
(43) Alberts, I. L.; Rowlands, T. W.; Handy, N. C. *J. Chem. Phys.* **1988**, *88*, 3811–3816.
(44) Aoyama, T.; Matsuoka, O.; Nakagawa, N. *Chem. Phys. Lett.* **1979**, *67*, 508–510.
(45) Bone, R. G. A.; Handy, N. C. *Theoretica Chimica Acta* **1990**, *78*, 133–163.
(46) Craw, J. S.; De Almeida, W. B.; Hinchliffe, A. *THEOCHEM* **1989**, *60*, 69–74.
(47) Prichard, D. G.; Nandi, R. N.; Muenter, J. S. *J. Chem. Phys.* **1988**, *89*, 115–123.
(48) Shuler, K.; Dykstra, C. E. *J. Phys. Chem. A* **2000**, *104*, 11522–11530.
(49) Shuler, K.; Dykstra, C. E. *J. Phys. Chem. A* **2000**, *104*, 4562–4570.
(50) Jovan Jose, K. V.; Gadre, S. R.; Sundararajan, K.; Viswanathan, K. S. *J. Chem. Phys.* **2007**, *127*, 104501/104501–104501/104510.
(51) Sundararajan, K.; Ramanathan, N. *J. Mol. Struct.* **2007**, *833*, 150–160.

JP806675N